

See discussions, stats, and author profiles for this publication at: <https://www.researchgate.net/publication/250917920>

# Clustered Geometries Exploiting Quantum Coherence Effects for Efficient Energy Transfer in Light Harvesting

ARTICLE in JOURNAL OF PHYSICAL CHEMISTRY LETTERS · JULY 2013

Impact Factor: 7.46 · DOI: 10.1021/jz4011477 · Source: arXiv

CITATIONS

10

READS

42

## 4 AUTHORS:



**Qing Ai**

Beijing Normal University

32 PUBLICATIONS 168 CITATIONS

SEE PROFILE



**Tzu-Chi Yen**

National Taiwan University

2 PUBLICATIONS 17 CITATIONS

SEE PROFILE



**Bih-Yaw Jin**

National Taiwan University

67 PUBLICATIONS 543 CITATIONS

SEE PROFILE



**Yuan-Chung Cheng**

National Taiwan University

34 PUBLICATIONS 917 CITATIONS

SEE PROFILE

# Clustered Geometries Exploiting Quantum Coherence Effects for Efficient Energy Transfer in Light Harvesting

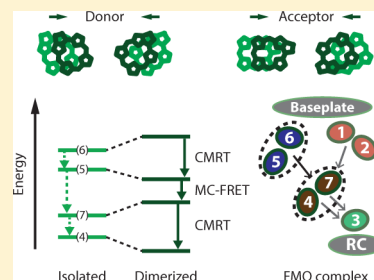
Qing Ai, Tzu-Chi Yen, Bih-Yaw Jin, and Yuan-Chung Cheng\*

Department of Chemistry and Center for Quantum Science and Engineering, National Taiwan University, Taipei City 106, Taiwan

**S** Supporting Information

**ABSTRACT:** Elucidating quantum coherence effects and geometrical factors for efficient energy transfer in photosynthesis has the potential to uncover nonclassical design principles for advanced organic materials. We study energy transfer in a linear light-harvesting model to reveal that dimerized geometries with strong electronic coherences within donor and acceptor pairs exhibit significantly improved efficiency, which is in marked contrast to predictions of the classical Förster theory. We reveal that energy tuning due to coherent delocalization of photoexcitations is mainly responsible for the efficiency optimization. This coherence-assisted energy-tuning mechanism also explains the energetics and chlorophyll arrangements in the widely studied Fenna–Matthews–Olson complex. We argue that a clustered network with rapid energy relaxation among donors and resonant energy transfer from donor to acceptor states provides a basic formula for constructing efficient light-harvesting systems, and the general principles revealed here can be generalized to larger systems and benefit future innovation of efficient molecular light-harvesting materials.

**SECTION:** Energy Conversion and Storage; Energy and Charge Transport



Photoactive molecular architectures have recently attracted intensive research interests in chemistry and nanoscience because of their potential to achieve extraordinary optoelectronic properties. For example, in natural photosynthesis, sophisticated pigment–protein complexes are responsible for absorbing light energy and transferring the excitation energy across tens of nanometers to the reaction center with near-unity quantum efficiency.<sup>1–5</sup> Inspired by these remarkable natural assemblies, artificial molecular systems have been synthesized to significantly improve the energy-transfer performance of organic materials.<sup>6,7</sup> Despite recent advances, the rational design of such photoactive molecular materials is still very much under development because a fundamental understanding of the structure–function relationships regarding excitation energy transfer (EET) and charge-transfer dynamics in these complex molecular systems in the condensed phase is still lacking.

Recently, quantum-beat-like phenomena observed in the two-dimensional electronic spectra of photosynthetic complexes<sup>8–10</sup> have inspired numerous research studies to understand the roles of quantum coherence in natural photosynthesis.<sup>11–16</sup> While the significance of coherent electronic dynamics in photosynthesis is still under debate,<sup>15,17–19</sup> it is clear that quantum effects are important, and recent works have provided much insight into the quantum mechanical control of energy transport,<sup>11,13,14,16,19–22</sup> including the significance of initial preparation.<sup>23,24</sup> We believe now that it is the time to go beyond detection and to confront the more relevant question in real-world applications, how to utilize electronic quantum coherence to build a more efficient EET network.

Before we go on to discuss coherence effects in EET, we believe that a more precise definition of coherence in excitonic systems is necessary. The term “coherence” generally refers to nonzero off-diagonal elements of the density matrix describing a quantum system. Because the values of a density matrix are basis-dependent, quantum coherence in EET phenomena could refer to different concepts.<sup>3,15</sup> In the site basis, in which electronic excitations localized on individual chromophores are used as the basis states, coherence represents coherent delocalization of excited states. In contrast, in the exciton basis, which includes delocalized eigenstates of the electronic Hamiltonian, coherence represents superposition of eigenstates, hence a nonstationary state that evolves coherently under the electronic Hamiltonian. It is clear that exciton delocalization plays an important role in the efficient harvesting of light energy in natural photosynthesis;<sup>4,25,26</sup> however, its connection to geometrical factors and EET efficiency have not been fully investigated. Therefore, in this work, we focus on the discussion of mechanisms related to exploiting exciton delocalization for efficient EET.

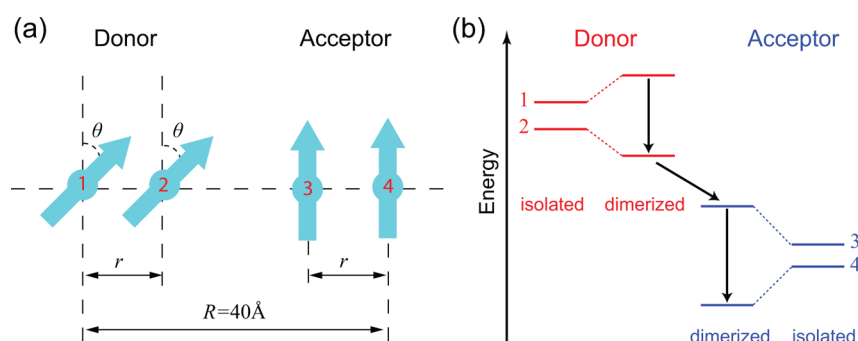
Regarding the design of efficient EET materials, the spatial arrangements of chromophores clearly are important variables. However, studies on the relationship between the spatial arrangement and EET efficiency in light harvesting have been sporadic. Schulten and co-workers have emphasized the importance of quantum coherence due to spatial closeness in affecting the spectral properties and functions of bacterial light-

**Received:** June 4, 2013

**Accepted:** July 19, 2013

**Published:** July 19, 2013

Scheme 1. (a) Schematic Diagram of the Four-Site Linear Model System<sup>a</sup> and (b) an Energy-Transfer Pathway between Donor and Acceptor Exciton States in the Four-Site Model<sup>b</sup>



<sup>a</sup>In the model, sites 1 and 2 form the donor pair, and sites 3 and 4 are the acceptor pair. The total distance between the two ends is fixed at  $R = 40 \text{ \AA}$ , while the intrapair distance ( $r$ ) and dipole tilt angle ( $\theta$ ) are varied to investigate geometrical effects. <sup>b</sup>The spectral overlap between the low-energy donor state and high-energy acceptor state can be enhanced by dimerization, leading to enhanced EET efficiency.

harvesting apparatus.<sup>25,27</sup> Sun and co-workers demonstrated that dimerization of bacteriochlorophylls in the ring-like light-harvesting complexes from purple bacteria leads to an enhanced efficiency for EET because of the symmetry properties of the eigenstates.<sup>28</sup> Furthermore, Buchleitner and co-workers studied EET efficiency of random networks of particles using a model with isotropic interactions and phenomenological incoherent hopping rates to discover properties of optimal EET networks.<sup>29,30</sup> Recently, Scholes and co-workers have investigated mechanisms for efficient EET between long-distance pairs of pigments in photosynthetic complexes from marine cryptophytes.<sup>9,31</sup> These works have provided much insight into the remarkable efficiency of natural light-harvesting systems; however, we still do not possess clear structural design principles for efficient EET systems.

Natural photosynthetic complexes often exhibit clusters of chromophores with strong electronic couplings between the cluster members,<sup>2</sup> and it has been proposed that these elements play important roles in the remarkable efficiency of natural light harvesting.<sup>15,32</sup> However, the mechanisms responsible for the efficiency enhancement (if there is any) in a clustered network and the role of electronic coherence in the process remain unclear. In this work, we aim to discover spatial arrangements of chromophores that can be used to exploit quantum coherence for efficient light harvesting. To this end, we investigate a simple linear network of four chromophores. Because of the simplicity, it allows us to directly elucidate geometrical factors and quantum coherence effects for the optimization of EET efficiency. We show that when exciton delocalization is considered, the spatial arrangement of the sites leading to optimal EET efficiency is different from what is predicted by a classical theory. As a result, we reveal new geometrical factors to improve the EET efficiency and molecular design via exciton delocalization. In addition, we argue that (1) an energy gradient toward the target site and (2) clustered arrangements of sites that utilize exciton delocalization to tune excitation energies and open up efficient EET pathways could be considered as two major factors in building an efficient EET system. Moreover, we show that these two principles can be applied to explain the design of the electronic Hamiltonian of the well-studied Fenna–Matthews–Olson (FMO) complex from green sulfur bacteria. In other words, instead of showing that the EET in FMO is efficient, we show how FMO is designed to have efficient EET.

In this work, we focus on electronic quantum coherence induced by coherent excitonic couplings between chromophores (sites).<sup>3,14,17,26</sup> It is interesting to note that there is emerging evidence that vibrational coherence could also play a significant role in photosynthesis.<sup>33–36</sup> Recently, Plenio and co-workers have proposed a vibrational spectral tuning principle for efficient EET.<sup>34</sup> Because their focus is on the design of environments (bath) while our focus is on the system's spatial arrangements of chromophores, we believe that our discovery is complementary to their findings. The combined results might lead to a full set of applicable rules for the molecular design of the environments (phonons) as well as the system for efficient EET materials.

We consider a model system with four chromophores in a linear geometry as depicted in Scheme 1a. The four sites consist of a pair of donors and a pair of acceptors determined by their relative site energies. Because it is well-known that a moderate energy gradient toward the energy sink contributes significantly in natural light-harvesting systems,<sup>4</sup> we choose to consider a case in which the two donor sites are higher in energy than the two acceptor sites. Therefore, the linear chain is effectively an energy wire that passes energy from one end to the other. To investigate the geometrical factors in EET, we fix the end-to-end distance of the system ( $R$ ) and vary the intrapair distance between the two donor (acceptor) sites ( $r$ ). In addition, we consider orientational dependence ( $\theta$ ) to take into account the dipole orientation effects. This four-site linear model, albeit a significant oversimplification, is not only one of the simplest EET systems that can exhibit electronic coherence effects but also a faithful representation of highly ordered molecular arrays in several synthetic systems.<sup>6,7</sup> By studying such a simplified model instead of a natural photosynthetic complex, we aim to clearly identify key geometrical factors contributing to efficient EET.

We model the four-site linear system using a Frenkel exciton Hamiltonian<sup>3,37</sup>

$$H_S = \sum_{j=1}^4 \epsilon_j |j\rangle \langle j| + \sum_{i \neq j} J_{ij} |i\rangle \langle j| \quad (1)$$

where  $|j\rangle$  describes the state with single excitation in the  $j$ th site,  $\epsilon_j$  denotes the site energy of  $|j\rangle$ , and the excitonic coupling  $J_{ij}$  is described by dipole–dipole interactions

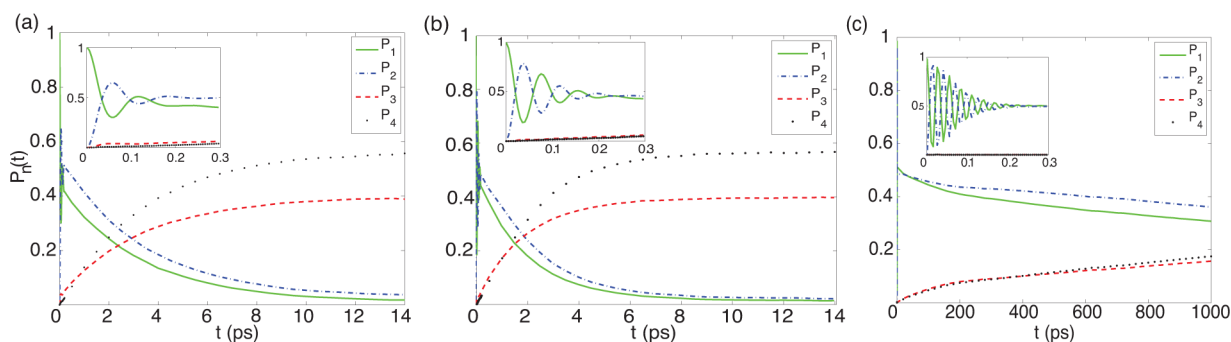


**Figure 1.** The EET dynamics of the four-site model calculated by the CMRT–NMQT method. The curves show populations of excitation on each of the four molecules in the system. Population dynamics for the geometry (a)  $r = 13.4$  Å and  $\theta = 0$ , (b)  $r = 11.4$  Å and  $\theta = 0$ , and (c)  $r = 8$  Å and  $\theta = 0$ . The insets display the coherent evolutions at the short times.

$$J_{ij} = \frac{1}{4\pi\epsilon_0 r_{ij}^3} [\vec{\mu}_i \cdot \vec{\mu}_j - 3(\vec{\mu}_i \cdot \hat{r}_{ij})(\vec{\mu}_j \cdot \hat{r}_{ij})] \quad (2)$$

where  $\vec{r}_{ij} = r_{ij}\hat{r}_{ij}$  is the displacement vector from site  $i$  to site  $j$ ,  $\vec{\mu}_i$  is the transition dipole of site  $i$ , and  $\epsilon_0$  is the vacuum permittivity. In our numerical simulations, we use the following parameters:  $\epsilon_1 = 13000$  cm<sup>−1</sup>,  $\epsilon_2 = 12900$  cm<sup>−1</sup>,  $\epsilon_3 = 12300$  cm<sup>−1</sup>,  $\epsilon_4 = 12200$  cm<sup>−1</sup>,  $\mu_j = 7.75$  D,  $R = 40$  Å,  $r = 6$ – $14$  Å, and  $T = 300$  K. To describe system–bath couplings, we consider independent harmonic baths coupled diagonally to the system described by Ohmic spectral density functions, as are normally used in the literature for photosynthetic complexes (more details about our model system and parameters are described in Appendix I in the Supporting Information). Here, we remark that *all of the parameters chosen in this study are in accordance with those in natural photosynthetic systems at ambient conditions.* Therefore, this model provides a realistic representation to shed light on the physical factors promoting efficient EET in photosynthetic systems. Note that we have also examined models with different site energies and intermolecular distances, and the results are only marginally different and do not affect the conclusions of this work.

Accurate simulations of the EET dynamics for the model system turn out to be a great challenge because of the broad parameter range spanned by varying  $r$  and  $\theta$ . By changing  $r$  and  $\theta$ , the intersite couplings ( $J_{ij}$ 's) vary significantly, effectively turning the system from the strong electronic coupling to weak electronic coupling limits. Among methods for EET dynamics accurate in a broad parameter range, the modified Redfield theory<sup>38,39</sup> yields reliable population dynamics of excitonic systems and has been successfully applied to describe spectra and population dynamics in many photosynthetic complexes.<sup>37,40–43</sup> Following the main idea of the modified Redfield theory, we consider the problem in the exciton basis and include the diagonal part of the exciton–bath interaction operator into the zeroth order Hamiltonian, while treating only the off-diagonal part of the exciton–bath interaction operator as the perturbation. We then derive the equations of motion for the full reduced density matrix of the excitonic system based on perturbative cumulant expansion up to the second order and the secular approximation to generalize the modified Redfield theory to treat time evolutions of off-diagonal terms in a density matrix,<sup>44</sup> providing a new theoretical approach for accurate descriptions of coherent EET dynamics. We thus apply this coherent modified Redfield theory (CMRT) to simulate the EET dynamics in this work. Note that although more accurate

nonperturbative methods are available,<sup>45–47</sup> they are not applicable in this case due to the need for numerical efficiency.

Incorporating the time evolution for the off-diagonal terms of the reduced density matrix in addition to dynamics of diagonal terms governed by the modified Redfield theory, the CMRT method provides a generalized quantum master equation (QME) for the reduced density matrix of an excitonic system in the exciton basis

$$\begin{aligned} \dot{\rho} = & -i \sum_{kk'} (\epsilon'_k - \epsilon'_{k'}) \rho_{kk'} |e_k\rangle \langle e_{k'}| \\ & + \sum_{k \neq k'} (R_{kk'}^{\text{dis}}(t) \rho_{k'k} |e_k\rangle \langle e_{k'}| - R_{kk'}^{\text{dis}}(t) \rho_{kk} |e_k\rangle \langle e_k|) \\ & - \sum_{k \neq k'} \left[ R_{kk'}^{\text{pd}}(t) + \frac{1}{2} \sum_{k'' (\neq k, k')} (R_{k''k}^{\text{dis}}(t) + R_{k''k'}^{\text{dis}}(t)) \right] \\ & \rho_{kk'} |e_k\rangle \langle e_{k'}| \end{aligned} \quad (3)$$

where  $\rho(t)$  is the density matrix with matrix element  $\rho_{kk'} = \langle e_k | \rho | e_{k'} \rangle$ ,  $|e_k\rangle$  is the  $k$ th eigen state of the electronic Hamiltonian  $H_s$ , and  $\epsilon'_k$  is the eigen energy of  $|e_k\rangle$  shifted by a reorganization energy due to the system–bath coupling. The expressions for time-dependent dissipation rates ( $R_{kk'}^{\text{dis}}(t)$ ) and pure dephasing rates ( $R_{kk'}^{\text{pd}}(t)$ ) are given in Appendix II in the Supporting Information. The CMRT has clear physical interpretation for each term. The three terms describe the coherent dynamics, the population dynamics, and the dephasing processes due to pure dephasing and population-transfer-induced decoherence, respectively. In addition, because we consider time-dependent rates, the CMRT QME is non-Markovian.

Furthermore, an efficient numerical simulation scheme is required as we need to calculate long-time dynamics of the four-site model with many different  $r$  and  $\theta$  in order to evaluate geometrical effects in the efficiency of light harvesting. To this end, we have adopted a non-Markovian quantum trajectory (NMQT) method<sup>48,49</sup> to provide efficient simulations of the CMRT dynamics. Specifically, direct propagation of the CMRT QME for a system with  $M$  sites requires solving  $M^2$  ordinary differential equations, whereas the NMQT method enables more efficient simulations of EET dynamics by unraveling the non-Markovian QME into  $M$  stochastic Schrödinger equations. Details on the unraveling of the CMRT QME and numerical algorithms for time propagation are given in Appendix III in the Supporting Information. Because the accuracy of the modified Redfield theory is well-validated for biased energy systems,<sup>37</sup>



the combined CMRT–NMQT approach provides an accurate and numerically efficient means to calculate coherent EET dynamics for general multilevel excitonic systems. Moreover, we have found that the NMQT simulation of the CMRT QME delivers additional numerical stability that is required to provide information about long-time EET dynamics governing the efficiency of EET.

We applied the combined CMRT–NMQT approach to investigate EET dynamics in the four-site model. To mimic the function of the system as a wire transferring energy from site 1 to site 4, we assume that site 1 is initially excited in all of our calculations. In Figure 1, we present calculated site population dynamics for the four-site model in three geometries with different intrapair distances. Figure 1a shows the EET dynamics of a system with equally spaced sites, that is,  $r = 13.4$  Å. In this case, the excitation energy moves coherently between sites 1 and 2 in  $\sim 300$  fs and then is transferred from the donor to the acceptor on a  $\sim 4$  ps time scale. Clearly, the combination of coherent energy relaxation within the donor pair and incoherent EET from the donor pair to the acceptor pair governs the whole EET process. Notably, this feature also appears in a broad range of models for natural light-harvesting systems.<sup>4,15</sup> Furthermore, we note that the combined CMRT–NMQT approach allows us to efficiently capture both the coherent dynamics at short times and the population decay at long times, while the original modified Redfield approach ignores the coherent dynamics, and as a result, it cannot be applied to describe the dynamics investigated here.

Figure 1b shows the EET dynamics of the four-site model with a reduced intrapair distance ( $r = 11.4$  Å). Compared to Figure 1a, EET from the donor to acceptor in this dimerized geometry is significantly more rapid ( $\sim 2$  ps). This result shows that the EET dynamics are sensitive to the geometry of the system, and the equally spaced geometry (Figure 1a) does not necessarily offer the best EET efficiency. Moreover, as the intrapair distance  $r$  is further decreased to a smaller value ( $r = 8$  Å, Figure 1c), the EET becomes extremely slow ( $\sim 7$  ns). Despite this, the oscillations in the short-time regime remain significant and even more pronounced due to stronger intrapair electronic coupling strengths. The results presented in Figure 1 indicate that an optimal geometry for EET exists, and the efficiency of EET is closely related to quantum coherence but not always positively correlated with the coherent evolution.

To quantify the efficiency of energy transfer across the four-site model system, we study the population at site 4 as a function of time,  $P_4(t)$ . As shown in Figure 1,  $P_4(t)$  generally exhibits a double-exponential behavior, with a rapid but minor rise and a major long-time exponential growth. Therefore, we fit  $P_4(t)$  to a double-exponential growth model and take the major rise component to define an effective end-to-end transfer rate  $R_{\text{eff}}$  (see Appendix IV in the Supporting Information). For the geometries studied in Figure 1, the effective transfer times  $\tau_{\text{eff}} = 1/R_{\text{eff}}$  obtained by fitting to  $P_4(t)$  are, respectively,  $\tau_{\text{eff}} =$  (a) 3.4, (b) 2.4, and (c) 6.9 ns.

In order to further investigate the relation between the EET efficiency and spatial arrangement of the sites, we simulate the EET dynamics of the four-site model for a broad range of intrapair distances  $r$  and dipole orientations  $\theta$  to obtain the effective end-to-end transfer rates  $R_{\text{eff}}$ . Figure 2a shows  $R_{\text{eff}}$  as a function of  $r$  and  $\theta$ . This map shows two optimal regions for the efficiency of EET across the linear four-site model near ( $\theta = 0, r = 11.3$  Å) and ( $\theta = 0.3\pi, r = 10.8$  Å), of which the intrapair distances are clearly smaller than the equally spaced value ( $r =$

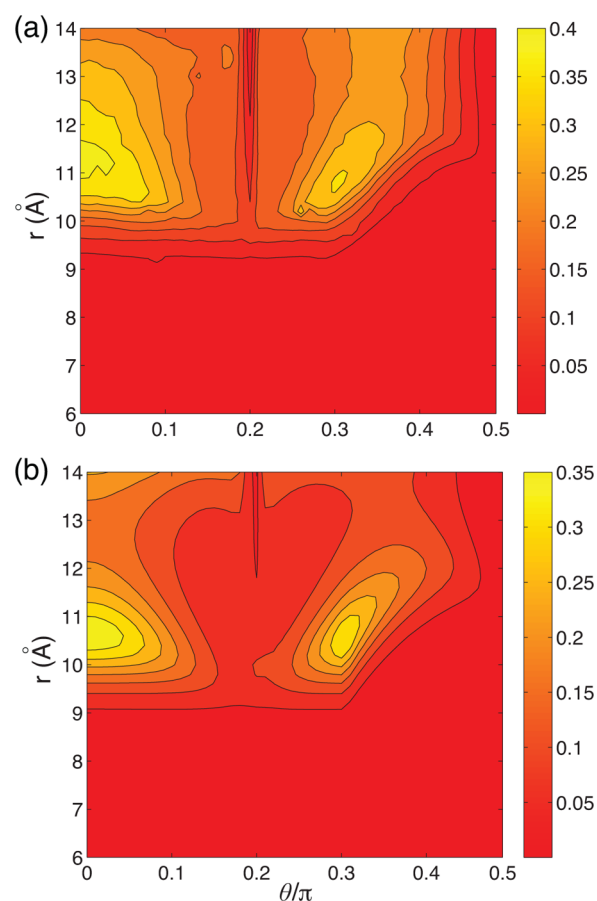


**Figure 2.** Geometrical dependence of the effective transfer rate  $R_{\text{eff}}$  ( $\text{ps}^{-1}$ ) as a function of the two geometrical parameters  $r$  and  $\theta$ . (a)  $R_{\text{eff}}$  calculated from full CMRT–NMQT dynamical simulations. (b)  $R_{\text{eff}}$  predicted by the analytical result in eq 5.

13.4 Å). This indicates that dimerized clusters offer enhanced transfer rates. For the optimal region at  $\theta = 0$ , the effective transfer rate increases to a maximum value as the distance is decreased to  $r = 11.3$  Å from the equally spaced value. As the distance is further decreased, the rate of energy transfer quickly decreases. This suggests that EET between the donor pair and the acceptor pair becomes crucial as the interpair distance becomes large.

The enhanced EET efficiency at dimerized geometries can be attributed to improved energy matching between donor and acceptor states due to increased intrapair electronic couplings. As illustrated in Scheme 1b, the exciton delocalization in the donor and acceptor pairs can shift eigen energies and reduce the energy gap between the lower-energy donor state and higher-energy acceptor state. When combined with rapid coherent equilibration of energy among the donor states, the enhanced energy matching leads to more efficient EET from the donor to the acceptor. Note that a classical sequential hopping picture of EET such as the Förster theory predicts that the equally spaced geometry would give rise to the optimal end-to-end EET efficiency because otherwise the slowest step would limit the transfer rate. What we have revealed here is an intrinsically quantum mechanical mechanism based on energy tuning due to exciton delocalization that gives rise to enhanced EET efficiency of a nontrivial dimerized geometry. We remark that the precise optimal geometry for EET depends on how the electronic couplings between sites are calculated. In our model,

we assume dipole–dipole interactions, which may not be valid in the short-distance regime. Nevertheless, more accurate estimations of electronic couplings should not change the prediction that dimerized clusters will give rise to enhanced EET efficiency in this particular geometry.

Regarding the dependence of  $R_{\text{eff}}$  on  $\theta$ , the situation becomes more complicated. In addition to the region around  $\theta = 0$  (parallel transition dipoles), there exists the other optimal region around  $\theta = 0.3\pi$  in Figure 2a. These two regions are separated by a minimum  $R_{\text{eff}}$  at around  $\theta \simeq 0.2\pi$ . To elucidate the orientational effects, we plot the magnitudes of the nearest-neighbor electronic couplings,  $J_{12}$ ,  $J_{23}$ , and  $J_{34}$ , as a function of  $\theta$  in Figure 3. There,  $J_{34}$  remains constant because the

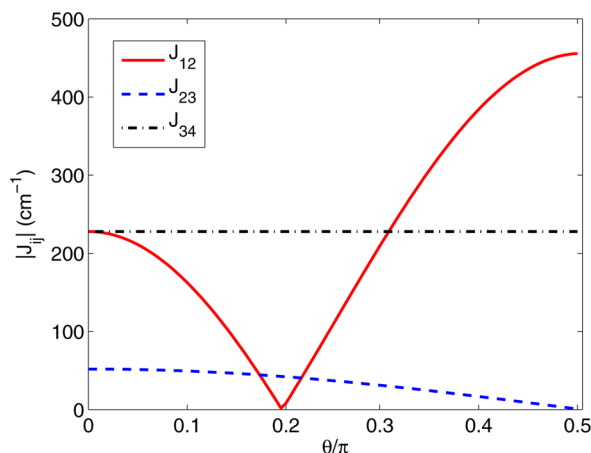


**Figure 3.** Magnitude of the calculated electronic coupling strengths  $|J_{ij}|$  as a function of  $\theta$  for  $r = 10.8$  Å. Here, we plot the three nearest-neighbor couplings as other couplings are much smaller. Note that because  $J_{12} < 0$  for  $\theta > 0.2\pi$ , the donor pair forms an H-aggregate when  $\theta < 0.2\pi$  and becomes a J-aggregate for  $\theta > 0.2\pi$ .

orientations of the two acceptor dipoles are fixed. In contrast,  $J_{23}$  slowly and monotonically decreases to zero as  $\theta$  increases from 0 to  $0.5\pi$ , while the dipoles of sites 2 and 3 change from a parallel orientation to a perpendicular orientation. Moreover,  $J_{12}$  not only changes its magnitude significantly but also its sign at  $\theta \simeq 0.2\pi$ , giving rise to a negligible  $J_{12}$  at around  $\theta = 0.2\pi$ . As a result of the vanishing  $J_{12}$ , energy transfer is strongly suppressed at  $\theta \simeq 0.2\pi$ , leading to the local minimum of  $R_{\text{eff}}$  in Figure 2a. Clearly, the optimal region at  $\theta = 0.3\pi$  is an interplay of the increase in the donor intrapair coupling ( $J_{12}$ ) and decrease in the interpair coupling ( $J_{23}$ ) as  $\theta$  passes  $0.2\pi$ . Finally, it is intriguing to note that the redistribution of transition dipoles due to electronic coherence also plays a minor role in the optimal region at  $\theta = 0.3\pi$  because the geometry corresponds to EET from a J-aggregate dimer to an H-aggregate dimer, indicating that enhanced transition dipole in the lower-energy state of the donor (J-type) and the higher-energy state of the acceptor (H-type) could further enhance the rate of donor-to-acceptor EET.

Figure 2a maps out the geometrical control factors of the effective transfer rate for the four-site model. What is the EET mechanism responsible for the geometrical dependence of EET efficiency? Does coherent evolution play a significant role in the optimal geometries? Can we establish a simple EET picture that accurately describes the dynamics in the broad parameter range covered in Figure 2a? To answer these questions and elucidate the key mechanisms of EET in the four-site model, we consider

EET in the system as a cascade energy relaxation involving three subprocesses (Scheme 1b),  $|e_1\rangle \rightarrow |e_2\rangle$ ,  $|e_2\rangle \rightarrow |e_3\rangle$ , and  $|e_3\rangle \rightarrow |e_4\rangle$ .

Due to the strong electronic coupling between the donor sites, there are significant populations distributed on both  $|e_1\rangle$  and  $|e_2\rangle$  when site 1 is initially excited. Therefore, two dominant energy relaxation pathways should be considered,  $|e_1\rangle \rightarrow |e_2\rangle \rightarrow |e_3\rangle$  and  $|e_2\rangle \rightarrow |e_3\rangle \rightarrow |e_4\rangle$ . The two relaxation processes compete with each other, and the overall transfer time is determined by the slower one, which is rate-determining. Consequently, if we assume that the transfer proceeds through exciton states in a sequential manner in the exciton basis, then the time required to complete the overall transfer process can be calculated from the rates of each individual step

$$\tau_{\text{total}} \simeq \max\{\tau_{2 \leftarrow 1} + \tau_{3 \leftarrow 2}, \tau_{3 \leftarrow 2} + \tau_{4 \leftarrow 3}\} \\ \simeq \max\left\{\frac{1}{R'_{21}} + \frac{1}{R'_{32}}, \frac{1}{R'_{32}} + \frac{1}{R'_{43}}\right\} \simeq \frac{1}{R'_{\text{eff}}} \quad (4)$$

where  $R'_{21}$ ,  $R'_{32}$ , and  $R'_{43}$  correspond to state-to-state EET rates of  $|e_1\rangle \rightarrow |e_2\rangle$ ,  $|e_2\rangle \rightarrow |e_3\rangle$ , and  $|e_3\rangle \rightarrow |e_4\rangle$ , respectively. As a result, we can estimate the effective transfer rate as

$$R'_{\text{eff}} \equiv \min\left\{\frac{R'_{21}R'_{32}}{R'_{21} + R'_{32}}, \frac{R'_{32}R'_{43}}{R'_{32} + R'_{43}}\right\} \quad (5)$$

To calculate the three relevant EET rates,  $R'_{21}$ ,  $R'_{32}$ , and  $R'_{43}$ , we opt for a combined modified Redfield and generalized Förster approach.<sup>43</sup> Because of the relatively strong dipole–dipole interactions within the donor and acceptor pairs, we calculate intrapair transfer rates  $R'_{21}$  and  $R'_{43}$  using the CMRT approach. On the other hand, due to the relatively weak interpair dipole–dipole interactions, the transfer rate from the donor to acceptor,  $R'_{32}$ , is calculated by the multichromophoric Förster resonance energy transfer (MC-FRET) theory.<sup>50</sup> As a result, we describe the EET processes in the dimerized four-site system as rapid relaxation within the respective donor and acceptor pairs described by CMRT and slower incoherent hopping of the exciton from the donor to acceptor described by the MC-FRET. We then use the calculated EET rates to estimate the effective transfer rate by eq 5 (see Appendix V in the Supporting Information).

The estimated rates are presented in Figure 2b. The excellent agreement of the estimated results to Figure 2a, which is obtained from full dynamical simulations, indicates that the combined CMRT/MC-FRET mechanism provides an excellent picture to describe the EET dynamics in the four-site model. We thus arrive at the conclusion that instead of the time-consuming full simulation of quantum dynamics, we could efficiently estimate the effective efficiency of the complete EET process by the combined CMRT/MC-FRET picture. Furthermore, in the analysis based on the combined CMRT/MC-FRET picture, eigenstates of the donor pair are used as the initial states for calculating the overall transfer rate determined by the slower process in the two-pathway model (Appendix V in the Supporting Information). Therefore, the excellent agreement between Figure 2a and b also indicates that although a localized initial state is used for propagating population dynamics by the combined CMRT–NMQT approach, the optimal geometries do not depend on such an initial preparation. In addition, because the estimated transfer rate is calculated from a purely incoherent picture of energy relaxation

in the delocalized exciton basis, the result indicates that coherence evolution does not play a significant role in the optimization of EET efficiency in this system. Note that this is likely related to the model system chosen here because coherent dynamics only contribute to rapid equilibrium within the donor pair and have negligible effects on the donor-to-acceptor EET process probed by the effective transfer rate. The coherently wired EET between long-distance pairs of pigments observed in photosynthetic complexes from marine cryptophytes<sup>9,31</sup> shows that the coherent dynamics could play an additional role in the optimization of EET efficiency. However, in this work, we only investigate how to use geometrical factors to exploit exciton delocalization for enhanced EET efficiency. It will be interesting to investigate geometries that can take advantage of coherent evolution in the future work.

Finally, what are the geometrical factors governing efficient EET in natural photosynthetic systems? Are the coherence-assisted principles revealed here applicable to the chlorophyll arrangements in photosynthetic complexes? Our calculations based on the four-site model suggest that a rapid EET can be achieved by (1) employing an energy bias toward the target site to create directional energy flow and (2) forming strongly coupled clusters to create exciton delocalization and tune exciton energies for better energy matching between the donor and acceptor cluster states. It is a common observation that natural photosynthetic complexes often exhibit moderate energy bias and clusters of chromophores,<sup>4,15,32</sup> which are fully consistent with our results. Moreover, the coherence-assisted energy tuning and energy bias clearly play crucial roles in the rapid EET in bacterial light-harvesting systems<sup>22,25,27</sup> and the long-range coherent energy transfer in cryptophytes.<sup>32,42</sup> In particular, the dimerization in the B850 ring of the light-harvesting system 2 (LH2) from purple bacteria leads to the spreading of the energy levels of the B850 states, which enables rapid energy transfer from B800 to upper B850 states.<sup>51</sup> In the following, we apply the two principles to shed light on the construction of the effective exciton Hamiltonian of the FMO complex from green sulfur bacteria.

The FMO complex exhibits remarkable energy-transfer efficiency that has become the subject of intensive research.<sup>11,21,23,52,53</sup> Figure 4a shows the pigment arrangement in a monomeric subunit of the FMO complex. FMO contains seven bacteriochlorophylls (BChls), and its function is to

conduct energy from the baseplate (close to BChls 1 and 6) to the reaction center (close to BChl 3). Therefore, it is conceivable that an energy gradient should exist to direct the energy flow from one end of the complex to the other end. Indeed, effective Hamiltonian models that were obtained from spectral fitting<sup>52,54</sup> and quantum chemistry calculations<sup>55</sup> all indicate that BChl 3 has the lowest transition energy, BChls 1, 2, 5, and 6 have higher energies, and the energies of BChls 4 and 7 are set in between (Figure 4b). Clearly, the site energies in FMO are tuned to form an energy funnel toward the reaction center. Noticeably, the energy of BChl 3 is significantly lower than those of all other sites. The large energy gap could support a highly localized exciton state and prevent back transfer, effectively generating a higher thermal population of excitation energy on BChl 3 for more efficiency EET to the reaction center. Thus, the site energies of BChls in FMO are fully consistent with the energy bias principle for enhancing EET efficiency.

In addition to site energies, electronic couplings can be varied by geometrical dimerization to improve energy matching of exciton states for efficient EET, and this is exactly the case in FMO. Pathway I shown in Figure 4b clearly illustrates the similarity to the dimerization scheme shown in Scheme 1b. There, BChls 5 and 6 are dimerized and so are BChls 4 and 7, leading to large intrapair electronic couplings (i.e., large  $J_{56}$  and  $J_{47}$ ) and delocalized excitations. As a result of the exciton delocalization caused by the enhanced couplings, the energy gap between the lower-energy exciton state of the BChls 5–6 dimer (donor) and the higher-energy exciton state of the BChls 4–7 dimer (acceptor) is reduced, which leads to increased spectral overlap and an enhanced EET rate from the donor to the acceptor according to MC-FRET. For the intrapair transfer, although the energy gap between two exciton states is increased, the energy transfer can still be rapid because intrapair energy relaxation between delocalized states follows the CMRT mechanism, which mainly depends on the spatial overlap of exciton states.<sup>3,37</sup> A similar mechanism can be used to describe pathway II, explaining the two primary EET pathways as have been revealed by 2D electronic spectroscopy.<sup>52,53</sup> We argue that the energy bias and exciton delocalization could account for the >90% of the quantum efficiency of FMO, while tuning of the vibrational environment (spectral density) and coherent evolution may provide efficiency optimization.<sup>11,14,16,21,24,34,35</sup> In other words, we have made clear two key underlying principles for the design of the effective Hamiltonian of FMO, and the control through spatial arrangements of BChls is apparent.

In summary, we have investigated the optimal spatial arrangements of chromophores for EET in a linear four-site model mimicking a coherent light-harvesting system. On the basis of combined CMRT–NMQT numerical simulations of EET dynamics, the geometrical factors affecting the end-to-end EET rate are investigated, and it is discovered that the effective transfer rate is maximized if the donor and acceptor sites are respectively dimerized in this given topology. Moreover, we also demonstrated that the dipole orientation angle  $\theta$  also plays an important role in the EET efficiency. This result is interesting and nontrivial because a classical approach such as the Förster resonance energy-transfer theory would predict that an equally spaced linear geometry should give rise to an optimal end-to-end transfer rate. Our analysis reveals that in contrast, exciton delocalization contributes crucially to the optimization of the energy-transfer efficiency. We conclude that coherence-

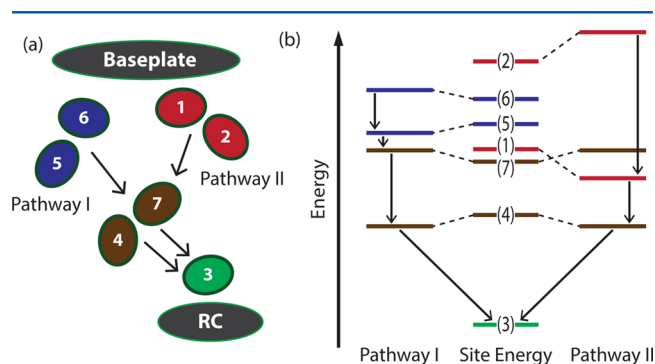


**Figure 4.** (a) Chlorophyll arrangement and EET pathways in the monomeric subunit of the FMO complex with respect to the baseplate and reaction center. (b) Excitation energy of each chlorophyll in FMO and the energetics of the exciton states.<sup>52</sup> Each of the two EET pathways is composed of a donor dimer and an acceptor dimer, similar to the four-site model studied in this work.



assisted energy tuning based on geometrical control of interchromophore electronic couplings provides a useful means to enhance EET efficiency. Furthermore, it is already well-known that a biased energy funnel to direct energy flow toward the target site also plays an important role in constructing efficient light-harvesting systems.<sup>4</sup> On the basis of these rules, the Hamiltonian of FMO is analyzed, and it is shown that the spatial arrangement of the seven BChls in combination with the site energy gradient favors efficient EET from the baseplate to the reaction center. In addition, we argue that FMO also makes use of exciton delocalization and dimerized BChl arrangements to optimize energy transfer. Although we have only investigated a simple linear system with small geometrical degrees of freedom, these principles could be generalized to larger systems. In Appendix VI in the Supporting Information, energy transfer in a ring-shaped six-site model is investigated to demonstrate that without an exception, clustered geometries also lead to optimal EET in such a nonlinear topology. Therefore, we believe that the basic principles revealed in this work may be generalized to larger molecular networks and benefit the future innovation of efficient artificial light-harvesting materials. Note that homogeneous systems such as chlorosomes or B850 rings of LH2 from purple bacteria belong to a different class of systems, in which additional symmetry-related rules might play more prominent roles in the optimization of EET rate.<sup>28,56,57</sup>

Finally, because we focus on the long-time dynamics in this work, the short-time coherent dynamics are overlooked, and an in depth investigation of the coherent evolution effects and geometrical factors might provide additional optimization rules for light harvesting.<sup>4,32</sup> In this regard, we believe that the combined CMRT–NMQT approach should provide a powerful theoretical tool for seeking optimal design of both natural and artificial light-harvesting systems because it yields accurate and efficient numerical simulations of coherent quantum dynamics for large excitonic systems.

## ■ ASSOCIATED CONTENT

### ■ Supporting Information

Details of the effective Hamiltonian and numerical parameters of the four-site model, brief introduction to the CMRT approach, description and numerical implementation of the CMRT–NMQT method, definition of the effective transfer rate, details of the two-pathway model for EET efficiency, and full calculation and analysis on the EET of a ring-shaped six-site model. This material is available free of charge via the Internet at <http://pubs.acs.org>.

## ■ AUTHOR INFORMATION

### Corresponding Author

\*E-mail: [yuanchung@ntu.edu.tw](mailto:yuanchung@ntu.edu.tw).

### Notes

The authors declare no competing financial interest.

## ■ ACKNOWLEDGMENTS

We thank stimulating discussions with J. Piilo, Y.-X. Hwangfu, Y.-J. Fan, and Y.-H. Liu. Q.A. thanks the National Science Council, Taiwan (Grant No. NSC 100-2811-M-002-162) for financial support. Y.C.C. thanks the National Science Council, Taiwan (Grant No. NSC 100-2113-M-002-004-MY2), National Taiwan University (Grant No. 101R891305), and Center for Quantum Science and Engineering (Subproject: 101R891401)

for financial support. We are grateful to the Computer and Information Networking Center, National Taiwan University for the support of high-performance computing facilities.

## ■ REFERENCES

- (1) Scholes, G. D.; Rumbles, G. Excitons in Nanoscale Systems. *Nat. Mater.* **2006**, *5*, 683–696.
- (2) Cogdell, R. J.; Gardiner, A. T.; Hashimoto, H.; Brotsudarmo, T. H. P. A Comparative Look at the First Few Milliseconds of the Light Reactions of Photosynthesis. *Photochem. Photobiol. Sci.* **2008**, *7*, 1150–1158.
- (3) Cheng, Y.-C.; Fleming, G. R. Dynamics of Light Harvesting in Photosynthesis. *Annu. Rev. Phys. Chem.* **2009**, *60*, 241–262.
- (4) Scholes, G. D.; Fleming, G. R.; Olaya-Castro, A.; van Grondelle, R. Lessons from Nature about Solar Light Harvesting. *Nat. Chem.* **2011**, *3*, 763–774.
- (5) Lambert, N.; Chen, Y.-N.; Cheng, Y.-C.; Li, C.-M.; Chen, G.-Y.; Nori, F. Quantum Biology. *Nat. Phys.* **2013**, *9*, 10–18.
- (6) Huang, Y.-S.; Yang, X.; Schwartz, E.; Lu, L. P.; Albert-Seifried, S.; Finlayson, C. E.; Koepf, M.; Kitto, H. J.; Ulgut, B.; Otten, M. B. J.; et al. Sequential Energy and Electron Transfer in Polysiocyanopeptide-Based Multichromophoric Arrays. *J. Phys. Chem. B* **2011**, *115*, 1590–1600.
- (7) Liu, K.-L.; Lee, S.-J.; Chen, I.-C.; Hsu, C.-P.; Yeh, M.-Y.; Luh, T.-Y. Ultrafast Energy Transfer in a Regioregular Silylene-Spaced Copolymer. *J. Phys. Chem. C* **2010**, *114*, 13909–13916.
- (8) Engel, G. S.; Calhoun, T. R.; Read, E. L.; Ahn, T. K.; Mancal, T.; Cheng, Y.-C.; Blankenship, R. E.; Fleming, G. R. Evidence for Wavelike Energy Transfer Through Quantum Coherence in Photosynthetic Systems. *Nature* **2007**, *446*, 782–786.
- (9) Collini, E.; Wong, C. Y.; Wilk, K. E.; Curmi, P. M. G.; Brumer, P.; Scholes, G. D. Coherently Wired Light-Harvesting in Photosynthetic Marine Algae at Ambient Temperature. *Nature* **2010**, *463*, 644–647.
- (10) Panitchayangkoon, G.; Hayes, D.; Fransted, K. A.; Caram, J. R.; Harel, E.; Wen, J.; Blankenship, R. E.; Engel, G. S. Long-Lived Quantum Coherence in Photosynthetic Complexes at Physiological Temperature. *Proc. Natl. Acad. Sci. U.S.A.* **2010**, *107*, 12766–12770.
- (11) Ishizaki, A.; Fleming, G. R. Theoretical Examination of Quantum Coherence in a Photosynthetic System at Physiological Temperature. *Proc. Natl. Acad. Sci. U.S.A.* **2009**, *106*, 17255–17260.
- (12) Mohseni, M.; Rebentrost, P.; Lloyd, S.; Aspuru-Guzik, A. Environment-Assisted Quantum Walks in Photosynthetic Energy Transfer. *J. Chem. Phys.* **2008**, *129*, 174106.
- (13) Chin, A. W.; Datta, A.; Caruso, F.; Huelga, S. F.; Plenio, M. B. Noise-Assisted Energy Transfer in Quantum Networks and Light-Harvesting Complexes. *New J. Phys.* **2010**, *12*, 065002.
- (14) Ishizaki, A.; Fleming, G. R. Quantum Coherence in Photosynthetic Light Harvesting. *Annu. Rev. Phys. Chem.* **2012**, *3*, 333–361.
- (15) Pachon, L. A.; Brumer, P. Computational Methodologies and Physical Insights into Electronic Energy Transfer in Photosynthetic Light-Harvesting Complexes. *Phys. Chem. Chem. Phys.* **2012**, *14*, 10094–10108.
- (16) Cao, J.; Silbey, R. J. Optimization of Exciton Trapping in Energy Transfer Processes. *J. Phys. Chem. A* **2009**, *113*, 13825–13838.
- (17) Scholes, G. D. Quantum-Coherent Electronic Energy Transfer: Did Nature Think of It First? *J. Phys. Chem. Lett.* **2010**, *1*, 2–8.
- (18) Fassioli, F.; Olaya-Castro, A.; Scholes, G. D. Coherent Energy Transfer under Incoherent Light Conditions. *J. Phys. Chem. Lett.* **2012**, *3*, 3136–3142.
- (19) Kassal, I.; Yuen-Zhou, J.; Rahimi-Keshari, S. Does Coherence Enhance Transport in Photosynthesis? *J. Phys. Chem. Lett.* **2013**, *4*, 362–367.
- (20) Rebentrost, P.; Chakraborty, R.; Aspuru-Guzik, A. Non-Markovian Quantum Jumps in Excitonic Energy Transfer. *J. Chem. Phys.* **2009**, *131*, 184102.
- (21) Wu, J.; Liu, F.; Shen, Y.; Cao, J.; Silbey, R. J. Efficient Energy Transfer in Light-Harvesting Systems, I: Optimal Temperature,



Reorganization Energy and Spatial-Temporal Correlations. *New J. Phys.* **2010**, *12*, 105012.

(22) Jang, S.; Cheng, Y.-C. Resonance Energy Flow Dynamics of Coherently Delocalized Excitons in Biological and Macromolecular Systems: Recent Theoretical Advances and Open Issues. *WIREs Comput. Mol. Sci.* **2013**, *3*, 84–104.

(23) Moix, J.; Wu, J.; Huo, P.; Coker, D.; Cao, J. Efficient Energy Transfer in Light-Harvesting Systems, III: The Influence of the Eighth Bacteriochlorophyll on the Dynamics and Efficiency in FMO. *J. Phys. Chem. Lett.* **2011**, *2*, 3045–3052.

(24) Wu, J.; Silbey, R. J.; Cao, J. Generic Mechanism of Optimal Energy Transfer Efficiency: A Scaling Theory of the Mean First-Passage Time in Exciton Systems. *Phys. Rev. Lett.* **2013**, *110*, 200402.

(25) Strümpfer, J.; Sener, M.; Schulten, K. How Quantum Coherence Assists Photosynthetic Light-Harvesting. *J. Phys. Chem. Lett.* **2012**, *3*, 536–542.

(26) Smyth, C.; Fassioli, F.; Scholes, G. D. Measures and Implications of Electronic Coherence in Photosynthetic Light-Harvesting. *Philos. Trans. R. Soc. London, Ser. A* **2012**, *370*, 3728–3749.

(27) Sener, M. K.; Strümpfer, J.; Hsin, J.; Chandler, D. E.; Scheuring, S.; Hunter, C. N.; Schulten, K. Förster Energy Transfer Theory as Reflected in the Structures of Photosynthetic Light-Harvesting Systems. *ChemPhysChem* **2011**, *12*, 518–531.

(28) Yang, S.; Xu, D. Z.; Song, Z.; Sun, C. P. Dimerization-Assisted Energy Transport in Light-Harvesting Complexes. *J. Chem. Phys.* **2010**, *132*, 234501.

(29) Scholak, T.; Wellens, T.; Buchleitner, A. Optimal Networks for Excitonic Energy Transport. *J. Phys. B* **2011**, *44*, 184012.

(30) Scholak, T.; de Melo, F.; Wellens, T.; Mintert, F.; Buchleitner, A. Efficient and Coherent Excitation Transfer Across Disordered Molecular Networks. *Phys. Rev. E* **2011**, *83*, 021912.

(31) Marin, A.; Doust, A. B.; Scholes, G. D.; Wilk, K. E.; Curmi, P. M. G.; van Stokkum, I. H. M.; van Grondelle, R. Flow of Excitation Energy in the Cryptophyte Light-Harvesting Antenna Phycocyanin 645. *Biophys. J.* **2011**, *101*, 1004–1013.

(32) Huo, P.; Coker, D. F. Theoretical Study of Coherent Excitation Energy Transfer in Cryptophyte Phycocyanin 645 at Physiological Temperature. *J. Phys. Chem. Lett.* **2011**, *2*, 825–833.

(33) Kolli, A.; O'Reilly, E. J.; Scholes, G. D.; Olaya-Castro, A. The Fundamental Role of Quantized Vibrations in Coherent Light Harvesting by Cryptophyte Algae. *J. Chem. Phys.* **2012**, *137*, 174109.

(34) del Rey, M.; Chin, A. W.; Huelga, S. F.; Plenio, M. B. Exploiting Structured Environments for Efficient Energy Transfer: The Phonon Antenna Mechanism. *J. Phys. Chem. Lett.* **2013**, *4*, 903–907.

(35) Chin, A. W.; Prior, J.; Rosenbach, R.; Caycedo-Soler, F.; Huelga, S. F.; Plenio, M. B. The Role of Non-equilibrium Vibrational Structures in Electronic Coherence and Recoherence in Pigment-Protein Complexes. *Nat. Phys.* **2013**, *9*, 1–6.

(36) Tiwari, V.; Peters, W. K.; Jonas, D. M. Electronic Resonance with Anticorrelated Pigment Vibrations Drives Photosynthetic Energy Transfer outside the Adiabatic Framework. *Proc. Natl. Acad. Sci. U.S.A.* **2013**, *110*, 1203–1208.

(37) Novoderezhkin, V. I.; van Grondelle, R. Physical Origins and Models of Energy Transfer in Photosynthetic Light-Harvesting. *Phys. Chem. Chem. Phys.* **2010**, *12*, 7352–7365.

(38) Zhang, W. M.; Meier, T.; Chernyak, V.; Shaul, M. Exciton-Migration and Three-Pulse Femtosecond Optical Spectroscopies of Photosynthetic Antenna Complexes. *J. Chem. Phys.* **1998**, *108*, 7763–7774.

(39) Yang, M.; Fleming, G. R. Influence of Phonons on Exciton Transfer Dynamics: Comparison of the Redfield, Förster, and Modified Redfield Equations. *Chem. Phys.* **2002**, *282*, 163–180.

(40) Novoderezhkin, V. I.; Rutkauskas, D.; van Grondelle, R. Dynamics of the Emission Spectrum of a Single LH2 Complex: Interplay of Slow and Fast Nuclear Motions. *Biophys. J.* **2006**, *90*, 2890–2902.

(41) Novoderezhkin, V. I.; Dekker, J. P.; van Grondelle, R. Mixing of Exciton and Charge-Transfer States in Photosystem II Reaction

Centers: Modeling of Stark Spectra with Modified Redfield Theory. *Biophys. J.* **2007**, *93*, 1293–1311.

(42) Novoderezhkin, V. I.; Doust, A. B.; Curutchet, C.; Scholes, G. D.; van Grondelle, R. Excitation Dynamics in Phycoerythrin 545: Modeling of Steady-State Spectra and Transient Absorption with Modified Redfield Theory. *Biophys. J.* **2010**, *99*, 344–352.

(43) Novoderezhkin, V.; Marin, A.; van Grondelle, R. Intra- and Inter-Monomeric Transfers in the Light Harvesting LHCII Complex: The Redfield–Förster Picture. *Phys. Chem. Chem. Phys.* **2011**, *13*, 17093–17103.

(44) Hwang-Fu, Y.-H.; Chen, Y.-T.; Cheng, Y.-C. Coherent Excitation Energy Transfer in Photosynthetic Light Harvesting: A Coherent Modified-Redfield Theory Approach. In preparation.

(45) Tanimura, Y. Stochastic Lionville, Langevin, Fokker–Planck, and Master Equation Approaches to Quantum Dissipative Systems. *J. Phys. Soc. Jpn.* **2006**, *75*, 082001.

(46) Jin, J.; Zheng, X.; Yan, Y. Exact Dynamics of Dissipative Electronic Systems and Quantum Transport: Hierarchical Equations of Motion Approach. *J. Chem. Phys.* **2008**, *128*, 234703.

(47) Ishizaki, A.; Fleming, G. R. Unified Treatment of Quantum Coherent and Incoherent Hopping Dynamics in Electronic Energy Transfer: Reduced Hierarchy Equation Approach. *J. Chem. Phys.* **2009**, *130*, 234111.

(48) Piilo, J.; Maniscalco, S.; Harkonen, K.; Suominen, K.-A. Non-Markovian Quantum Jumps. *Phys. Rev. Lett.* **2008**, *100*, 180402.

(49) Piilo, J.; Harkonen, K.; Maniscalco, S.; Suominen, K.-A. Open System Dynamics with Non-Markovian Quantum Jumps. *Phys. Rev. A* **2009**, *79*, 062112.

(50) Jang, S.; Newton, M.; Silbey, R. Multichromophoric Förster Resonance Energy Transfer. *Phys. Rev. Lett.* **2004**, *92*, 218301.

(51) Yen, T.-C.; Cheng, Y.-C. Electronic Coherence Effects in Photosynthetic Light Harvesting. *Procedia Chem.* **2011**, *3*, 211.

(52) Cho, M.; Vaswani, H. M.; Brixner, T.; Stenger, J.; Fleming, G. R. Exciton Analysis in 2D Electronic Spectroscopy. *J. Phys. Chem. B* **2005**, *109*, 10542–10556.

(53) Brixner, T.; Stenger, J.; Vaswani, H. M.; Cho, M.; Blankenship, R. E.; Fleming, G. R. Two-Dimensional Spectroscopy of Electronic Couplings in Photosynthesis. *Nature* **2005**, *434*, 625–628.

(54) Adolphs, J.; Renger, T. How Proteins Trigger Excitation Energy Transfer in the FMO Complex of Green Sulfur Bacteria. *Biophys. J.* **2006**, *91*, 2778–2797.

(55) Mueh, F.; Madjet, M. E.-A.; Adolphs, J.; Abdurahman, A.; Rabenstein, B.; Ishikita, H.; Knapp, E.-W.; Renger, T. Alpha-Helices Direct Excitation Energy Flow in the Fenna–Matthews–Olson Protein. *Proc. Natl. Acad. Sci. U.S.A.* **2007**, *104*, 16862–16867.

(56) Kim, J.-H.; Cao, J. Optimal Efficiency of Self-Assembling Light-Harvesting Arrays. *J. Phys. Chem. B* **2010**, *114*, 16189–16197.

(57) Cleary, L.; Chen, H.; Chuang, C.; Silbey, R. J.; Cao, J. Optimal Fold Symmetry of LH2 Rings on a Photosynthetic Membrane. *Proc. Natl. Acad. Sci. U.S.A.* **2013**, *110*, 8537–8542.